BASIC RESEARCH www.jasn.org

Podocin Participates in the Assembly of Tight Junctions between Foot Processes in Nephrotic Podocytes

Akemi Shono,* Hiroyasu Tsukaguchi,* Eishin Yaoita,† Masaaki Nameta,‡ Hidetake Kurihara,§ Xiao-Song Qin,* Tadashi Yamamoto,† and Toshio Doi*

*Department of Clinical Biology and Medicine, University of Tokushima Graduate School of Medical Sciences, Tokushima, †Department of Structural Pathology, Institute of Nephrology, Graduate School of Medical and Dental Sciences, and ‡Cooperative Laboratory for Electron Microscopy, Niigata University, Niigata, and §Department of Anatomy, Juntendo University School of Medicine, Tokyo, Japan

ABSTRACT

The predominant type of cellular junction between normal podocyte foot processes is the slit diaphragm. Under nephrotic conditions,however, foot process effacement leads to the loss of slit diaphragms and the new formationof tight junctions composed of the proteins coxsackievirus and adenovirus receptor (CAR) and zonula occludens 1 (ZO-1). Podocin, a protein that plays a key role in maintaining the integrity of the slit diaphragm, has also been localized to these tight junctions, but its function at this site is unknown. In this study, we confirmed that podocin colocalizes with CAR and ZO-1 at the tight junction between foot processes in nephrotic rats. Using primary cultures of rat podocytes, as well as cell lines that co-expressed podocin and CAR, we observed that podocin was recruited to sites of cell–cell contact and that it co-localized with CAR and ZO-1. Immunoprecipitation suggested that these three junctional proteins from a multi-protein complex. Consistent with this, we found that podociin facilitated the coalescence of preassembled lipid rafts containing CAR and restricted their lateral mobility, the latter likely a result of dynamic actin reorganization and subsequent tethering of CAR-podocin complexes to the cytoskeleton. In conclusion, in addition to serving as a structural protein of the slit diaphragm of normal podocytes, our data suggest that podocin may also serve as a scaffold that links tight junction proteins to the actin cytoskeleton in nephrotic foot processes.

J Am Soc Nephrol 18: 2525–2533, 2007. doi: 10.1681/ASN.2006101084

The slit diaphragm (SD) is maintained by multiple molecular interactions that ensure stable anchorage of the membrane complexes to the actin cytoskeleton.[1,2] Several podocyte proteins play a key role in the maintenance of SD integrity. Nephrin is a transmembrane protein with eight Ig-like domains and constitutes a major structural backbone of the SD.[3] Podocin is a 42-kD integral membrane protein that interacts with nephrin at the SD.[4,5] It has a hairpin-like structure, the membrane topology of which is reminiscent of caveolin.[6] Similar to caveolin, podocin is present in high-order oligomeric complexes and localizes in so-called "rafts," the specialized membrane microdomains where sphingolipids and cholesterol are highly enriched.[5,7] The multiprotein SD complexes are assembled through the rafts.[8]

There are two types of cellular junctions in the foot process: SD and tight junction (TJ).[9,10] TJ is defined by the morphologic features of fusion points on the op-

Received October 3, 2006. Accepted May 22, 2007.

Published online ahead of print. Publication date available at www.jasn.org.

Correspondence: Dr. Hiroyasu Tsukaguchi, Department of Clinical Biology and Medicine, The University of Tokushima Graduate School of Medical Sciences, 3-18-15 Kuramoto, Tokushima, 770-0042, Japan. Phone: +81-88-633-7184; Fax: +81-88-633-9245; E-mail: hiroyasu@clin.med.tokushima-u.ac.jp

posing membranes. The characteristics are distinguishable from SD that forms the junctions with the usual 20- to 50-nm intercellular gap. In normal foot processes, the SD constitutes a major cellular junction, whereas the TJ is rarely encountered. Under nephrotic conditions of human[11] and rat,[9] the TJ complex newly appears at the interface of foot processes as it replaces the vanishing SD and/or emerges below the apically dislocated SD.[9,12] The TJ complex represents immature assembly that evolves into the SD during glomerular development, and these two junctions share the common structural element zonula occludens-1 (ZO-1), a cytosolic scaffold protein.[10] Studies in rats with puromycin aminonucleoside (PAN) nephrosis revealed that coxsackievirus and adenovirus receptor (CAR), a transmembrane protein with two extracellular Ig-like domains, serves as a TJ component in nephrotic foot processes.[13] Besides the originally identified function as a virus receptor,[14] CAR serves as a TJ protein that links the adhesion complexes to F-actin through interaction with ZO-1.[15]

Localization of podocin at the TJ complex has reportedly been observed,[16] but the biologic relevance and underlying molecular basis remain to be elucidated. These observations led us to explore whether podocin is implicated in TJ complex formation. In this study, we investigated the role of podocin in TJ complex by focusing on the interaction with a new binding partner CAR and ZO-1.

RESULTS

Podocin Co-localizes with CAR at the TJ-Like Structures in PAN Glomeruli

Ultrastructural analysis of normal rat glomeruli demonstrated that the vast majority of podocin is primarily localized at the cytoplasmic face of the plasma membrane adjacent to the SD. In contrast, CAR was not found anywhere in the foot process, with the exception of the TJ-like structures that were only rarely encountered under normal conditions. ZO-1 was concentrated along the cytoplasmic surfaces of the SD in association with podocin (data not shown). In PAN glomeruli at day 4, CAR accumulated exclusively at TJ-like structures between adjacent foot processes but was rarely located at the SD (Figure 1, A through D). In contrast, podocin became more frequently co-localized with CAR at sites of cell–cell contacts in opposing foot processes, whereas some podocin remained in its usual position at the SD. Quantification revealed that podocin distributes to the SD and TJ-like structures in almost equal frequency (Table 1). In PAN glomeruli at day 11 (Figure 1, E through I), podocin and CAR accumulated along the regions of close contact between adjacent foot processes, where ZO-1 co-distributed. These data suggest that CAR is preferentially involved in the formation of TJ complexes but not SD, whereas podocin is implicated in the assembly of both SD and TJ complexes.

Podocin Is Recruited to the Cell–Cell Junctions in Cultured Cells

In COS-7 cells co-expressing CAR and podocin, both proteins

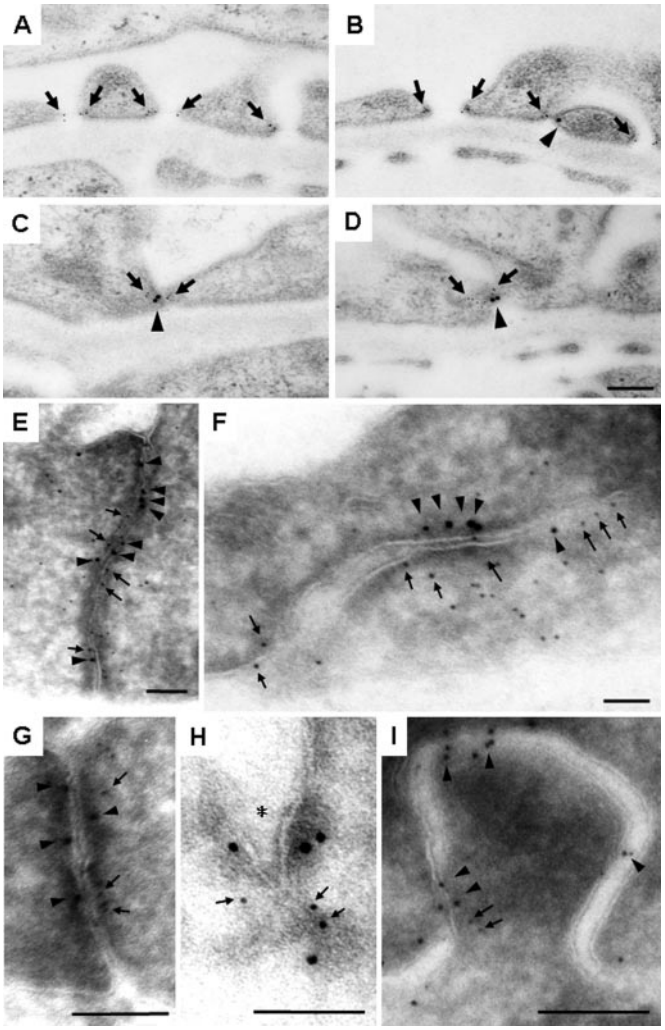

Figure 1. Podocin localizes to various junctions in nephrotic foot processes. (A through D) Double-immunogold staining of ultrathin sections from the periodate-lysine-paraformaldehyde–fixed rat glomeruli at 4 d after puromycin aminonucleoside (PAN) injection. There are a series of intercellular junctions with varying gap distance: Normal slit (A), tight junctions between adjoining foot processes (C and D), and both (B). Podocin (arrow, 5 nm gold) and coxsackievirus and adenovirus receptor (CAR; arrowhead, 15 nm gold) are depicted. Bar = 0.2 μm. (E and F) Cryosections of rat glomeruli at 11 d after PAN injection are double labeled with zonula occludens-1 (ZO-1; arrows, 5 nm gold) and CAR (arrowheads, 10 nm gold). Note that CAR preferentially localizes along the regions of close contact between adjacent foot processes. Bar = 0.1 μm. (G through I) Cryosections of rat glomeruli on PAN 11 are double labeled with ZO-1 (arrows, 5 nm gold) and podocin (arrowheads, 10 nm gold). *Apically dislocated slit diaphragm (SD). Note that podocin distributes to both shifted SD and tight junction (TJ)-like structures. Bar = 0.1 μm. Expression of CAR upregulated by approximately four-fold at 4 d after PAN injection, whereas that of podocin did not significantly alter during 10 d (Supplementary Figure 1).

Table 1. Frequency of immunogold-positive junctions of nephrotic foot processes[a]

Parameter	Frequency of Labeled Junctions (%)[b]		Gold Particles Associated with Cell–Cell Junctions (%)[c]
	SD	TJ-Like Junctions	
CAR	ND	35.6 ± 10.4	97.5 ± 5.0
Podocin	68.8 ± 8.6	66.4 ± 16.6	92.7 ± 8.2

[a]Ultrathin sections of rat glomeruli at day 4 after puromycin aminonucleoside injection were double labeled for podocin and coxsackievirus and adenovirus receptor (CAR) by gold particles of 5 and 15 nm, respectively, as described in the Concise Methods section. ND, not detectable; SD, slit diaphragm; TJ, tight junction.

[b]Frequency of podocin- or CAR-labeled junctions *versus* nonlabeled ones is shown as a percentage in total of 50 to 100 of SD or TJ-like structures (mean ± SEM from six independent experiments). The cell–cell junctions that had a discrete gap (>20 nm) are designated as SD, whereas those with no visible intercellular space are called TJ-like structures.

[c]Frequency of immunogold particles accumulating at cell–cell junctions (either SD or TJ-like structures) *versus* at the reminder locations is shown as a percentage of total number of foot process–associated gold marks (n = 100 to 200). The criteria that discriminate junctional labelings from those locating anywhere else in the foot process cytoplasm are according to Wernerson *et al.* (*Nephrol Dial Transplant* 18: 70–76, 2003). Data are means ± SEM from six independent experiments.

primarily exhibit a diffuse punctate pattern throughout the cytoplasm, although some expression also is distributed along the edge of the cell as well (Figure 2A). The quantification of intracellular vesicles revealed that 30 to 40% of podocin-positive puncta co-localize with CAR-labeled spots and *vice versa* (Figure 2B), suggesting that a significant proportion of the two proteins may be sorted into the same vesicles. It is notable that podocin is remarkably concentrated along cell–cell borders when neighboring cells came into contact (Figure 2A). A similar distribution of podocin was observed for primary cultured podocytes (Figure 2C), showing that the endogenous podocin was expressed at sites of cell–cell contacts, at which ZO-1 concomitantly accumulated. However, podocin was virtually absent at the cellular free edges. These observations suggested that cell–cell attachment is required for translocation of podocin to the cell–cell interface. When MDCK cells co-expressing CAR and podocin were sparsely plated at a lower density, both proteins showed a diffuse cytoplasmic punctate vesicle pattern. Once these cells came into cell contact and acquired cell polarity, both CAR and podocin concentrated focally at the points of cell–cell contacts with ZO-1 (Figure 2D). The data indicate that a proportion of podocin is recruited to cell–cell contacts in association with CAR and ZO-1.

Podocin Physically Interacts with the TJ Markers

Immunoprecipitation assays revealed that podocin co-precipitated with CAR in lysates from CAR and podocin co-expressing COS-7 cells and *vice versa* (Figure 3A). Pull-down assays with lysates from COS-7 cells and rat glomeruli revealed that at least the last C-terminal 65 amino acids of CAR are essential to mediate the interaction with podocin (Figure 3, B and C) and that the C-terminal 122 amino acids of podocin are crucial for the binding to CAR (Figure 3, D and E). Endogenous ZO-1 co-precipitated podocin as a complex from COS-7 cells expressing podocin (Figure 3F) and also co-precipitated CAR from those expressing CAR (Figure 3G). In reciprocal experiments, podocin and CAR co-precipitated endogenous ZO-1. These data indicate that podocin physically interacts with CAR and ZO-1 and forms a multiprotein complex, through either a direct or an indirect association in these cells.

CAR Interacts with Podocin through Lipid Rafts

Antibody cross-linking is a reliable technique that allows detection of even weak association to the rafts.[17,18] Upon antibody-induced cross-linking, CAR preferentially co-patched with the raft marker ganglioside GM1 (labeled by Cholera toxin B subunit, 39.8 ± 8.3%; n = 5) rather than the nonraft marker transferrin receptor TfR del 4 to 51 (21.2 ± 7.3%; n = 6; Figure 4, A through D and G). The cholesterol-depleting agent methyl β cyclodextrin inhibited antibody-induced clustering of CAR (data not shown), indicating that CAR forms a large cluster in a cholesterol-dependent manner. When CAR-podocin co-expressing COS-7 cells were cross-linked, podocin co-localized with clustered CAR at the cell surface (Figure 4, E and F), but coexpression of podocin *per se* did not further augment the extent of co-localization of CAR with the raft marker GM1 (39.8 ± 8.3% without podocin *versus* 40.3 ± 7.2% with podocin; n = 4 to 6; Figure 4G). The results indicate that CAR clusters *via* a raft-mediated mechanism and that podocin supports the coalescence of preexisting small rafts containing CAR.

Podocin Enhances Raft Association and Oligomerization of CAR

We examined the biochemical property of detergent-resistant membrane containing CAR.[19] The floating analysis with lysate from COS-7 cells and isolated rat glomeruli revealed a remarkable partitioning of CAR into cholesterol-rich fractions (Figure 5 and Supplementary Figure 2). Clustering and oligomerization of raft proteins reportedly promote the coalescence of more rafts and thereby stabilize the microdomains.[17] We therefore investigated the effects of podocin coexpression and antibody cross-linking on raft association of CAR. Antibody cross-linking of CAR or podocin coexpression alone led to a slight increase in raft association of CAR of 1.2-fold (32.7 ± 6.2%; n = 2) and 1.8-fold (48.4 ± 2.4%; n = 3), respectively, compared with control (26.3 ± 3.2%; n = 5; Figure 6, A and B). However, the combination of cross-linking and podocin coexpression resulted in increased CAR floating to the rafts (69.3 ± 1.2% *versus* control; $P < 0.01$; n = 5; Figure 6, A and B). Continuous sucrose gradient ultracentrifugation analysis demon-

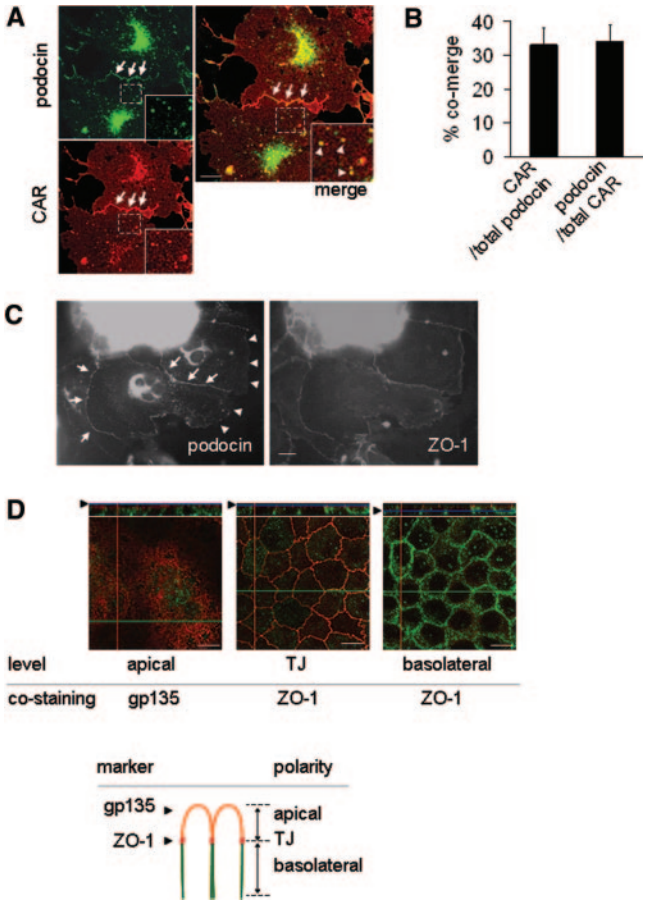

Figure 2. Podocin is recruited to the cell–cell junctions and co-localizes with CAR and ZO-1. (A) Double labeling of CAR (red) with podocin (green) in transiently transfected COS-7 cells. Both CAR and podocin co-localize in the cytoplasmic vesicles (arrowheads) and preferentially concentrate along cell–cell contacts (arrows). (B) Proportion of a CAR–podocin double-labeled cytoplasmic vesicle within the total number of intracellular vesicles expressing either CAR or podocin is presented. Bar = 10 μm. Results are representative of three independent experiments. (C) Primary cultured podocytes migrating from the decapsulated rat glomeruli. Podocin co-localizes with ZO-1 along cell–cell contacts (arrows) and not at the cellular free edges (arrowheads). Bars = 10 μm. CAR co-merges with ZO-1 along cell–cell contacts (data not shown). (D) Polarized epithelial MDCK cells stably expressing podocin. A series of sections are shown at the apical portion (marker gp135, red), at the TJ (marker ZO-1, red), and at the basolateral portion underneath the TJ (co-staining with ZO-1, red). (Top) Vertical section view. Podocin (green) localizes broadly alongside the basolateral membrane and accumulates focally at the cell–cell contacts with ZO-1. Note that no podocin staining is seen on the apical membrane. Bars = 10 μm.

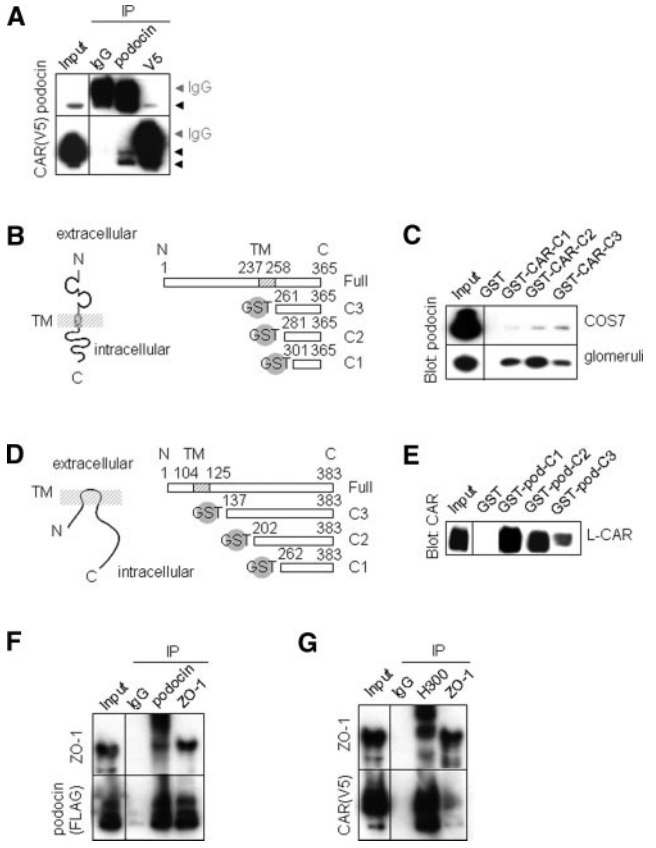

Figure 3. Podocin interacts with CAR and ZO-1. (A) Podocin and V5-tagged CAR co-immunoprecipitate each other. Lysates from COS-7 cells coexpressing V5-tagged CAR and podocin were precipitated with a control IgG or indicated antibodies. Arrowheads mark the immunoprecipitation products. IgG, IgG heavy chains. Membrane topology of CAR (B) and podocin (D). TM, transmembrane domain. (C) The C-terminus of CAR interacts with podocin. GST pull-downs using lysates from podocin-expressing COS-7 cells and rat glomeruli reveal that CAR binds podocin through its C-terminus. (E) The C-terminus of podocin is associated with CAR. GST pull-down assay using lysates from L cells stably expressing CAR (L-CAR) shows that the C-terminus of podocin interacts with CAR. (F and G) CAR and podocin interact with endogenous ZO-1 and *vice versa*. Lysates from COS-7 cells expressing either FLAG-tagged podocin (F) or V5-tagged CAR (G) are immunoprecipitated with a control IgG or polyclonal antibodies against podocin, CAR (H300), and ZO-1.

strated that both podocin and CAR form oligomers in high-order complex (Figure 6C; data not shown for podocin). Podocin coexpression led to a slight shift of CAR into the higher molecular weight fraction ($n = 5$; $P < 0.05$; Figure 6, C and D). Our data indicate that CAR ectodomain engagement and podocin coexpression cooperatively enhance raft partitioning of CAR by promoting its oligomerization.

Podocin Restricts the Diffusional Mobility of CAR in Living Cells

We next examined the diffusion property of green fluorescence protein (GFP)-tagged CAR (Figure 7A) in living cells by fluorescence recovery after photobleaching. Mouse L cells stably expressing podocin (L-pod) were used to ensure equal abundance of podocin for each experiment. Wild-type L cells (L-wt)

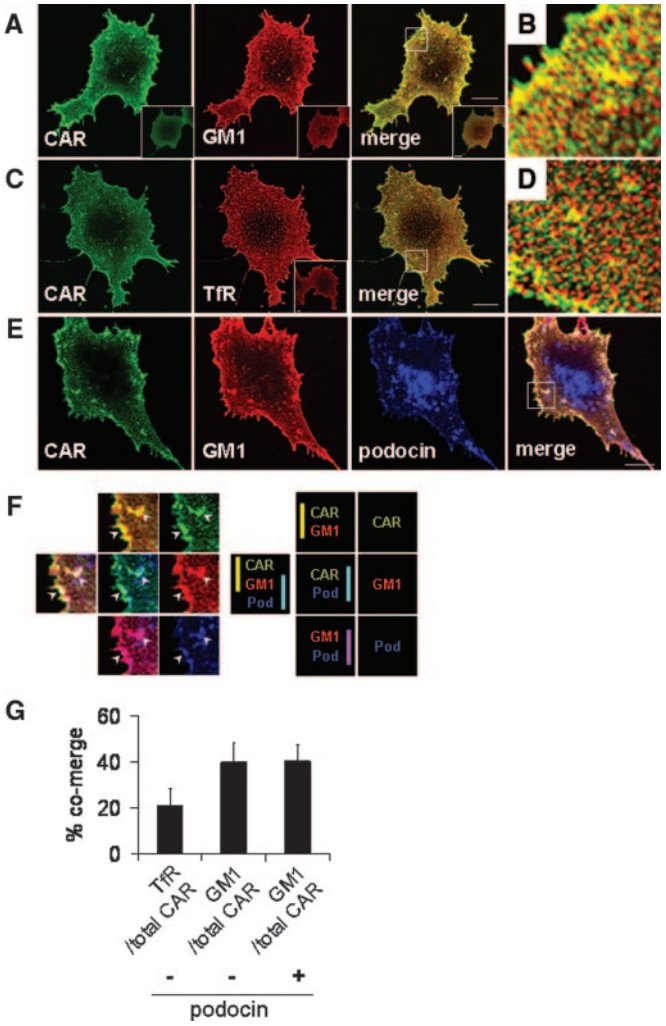

Figure 4. Clustered CAR preferentially partitions in lipid rafts in living cells. Surface of COS-7 cells expressing CAR alone (A) and of those coexpressing CAR and V5-tagged transferrin receptor (TfR; C) is cross-linked by anti-RmcB mAb, Cholera toxin B subunit (CT-B) biotin, and anti-V5 polyclonal antibodies. (Insets) Non–cross-linked control. (B and D) Higher magnification of boxed regions in A and C, respectively. Cross-linked CAR (green) co-patches with the raft marker GM1 (B) but co-patches to a lesser degree with the nonraft marker TfR (D). (E) Clustered CAR co-patches with GM1 and podocin. (F) Higher magnification of boxed portion in E. Arrowheads indicate discrete spots where CAR, podocin, and GM1 co-localize. (G) Proportion of CAR that co-merges with the raft or nonraft markers is quantified. CAR co-clusters more frequently with GM1 than with TfR. Bars = 10 μm.

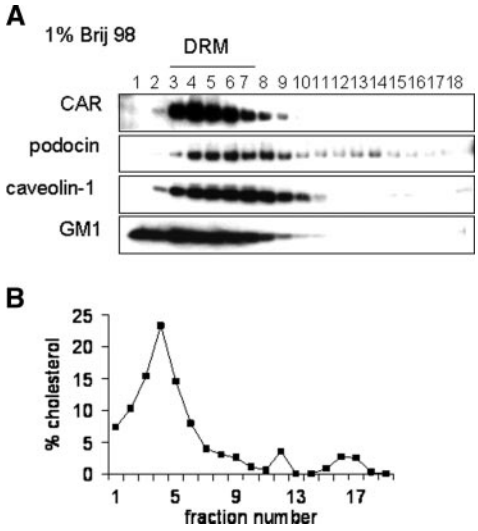

Figure 5. Podocin and CAR partition into the raft fractions in COS-7 cells. (A) Floating assay using 1% Brij 98 extracted lysates from COS-7 cells coexpressing CAR and podocin reveals that CAR and podocin co-fractionate to the low-density, detergent-resistant membrane (DRM) fractions with the raft marker of caveolin-1 and GM1. (B) Cholesterol content in each fraction is shown as a proportion in the total amount from all fractions. The preliminary data indicated that CAR has a considerably weaker affinity to rafts than nephrin or podocin and that the Brij 98 is a suitable detergent for the floating assay (Supplementary Figure 3).

or the L-pod were transiently transfected with GFP-CAR, and fluorescence recovery was compared between L cells expressing GFP-CAR alone (L-wt GFP-CAR) and those coexpressing GFP-CAR and podocin (L-pod GFP-CAR). As shown in Figure 7, B and C, in L-wt expressing GFP-CAR (L-wt GFP-CAR), fluorescence intensity reached a plateau of 83.8 ± 12.2% of the prebleached value with a recovery time of 300 s ($n = 6$). In contrast, L-pod GFP-CAR displayed a significantly higher percentage of the immobile fraction (47.0 ± 9.5%) than L-wt GFP-CAR (16.2 ± 12.2%; $P < 0.001$; $n = 6$; Figure 7D). These data indicate that podocin confines the lateral mobility of CAR in a living plasma membrane.

Clustering of CAR Leads to the Redistribution of F-actin and Podocin

The restricted lateral diffusion of surface proteins may be due in part to their tethering to the actin cytoskeleton.[20] To test this hypothesis, we examined the effects of CAR ectodomain engagement on the distribution of F-actin and podocin. In CAR-podocin coexpressing COS-7 cells, antibody-mediated clustering of CAR resulted in rearrangement of the actin cytoskeleton from its original filament-like pattern to a larger discrete punctate spot (Figure 8, A and B)—a morphologic pattern similar to the "actin comets" that represent the sites of dynamic actin reorganization.[20] Notably, phalloidin staining indicated that the focal accumulation of F-actin coincided with the patches where CAR and podocin co-localized (Figure 8A). Quantitative analysis revealed that podocin coexpression with CAR further increases the proportion of cells exhibiting actin filament reorganization (Figure 8C). However, an actin co-sedimentation assay with COS-7 cells showed that podocin does not alter the binding affinity of CAR to F-actin (Supplementary Figure 4). Taken together, these data suggest that clustering of CAR induces focal cytoskeletal responses in association with podocin (Figure 9).

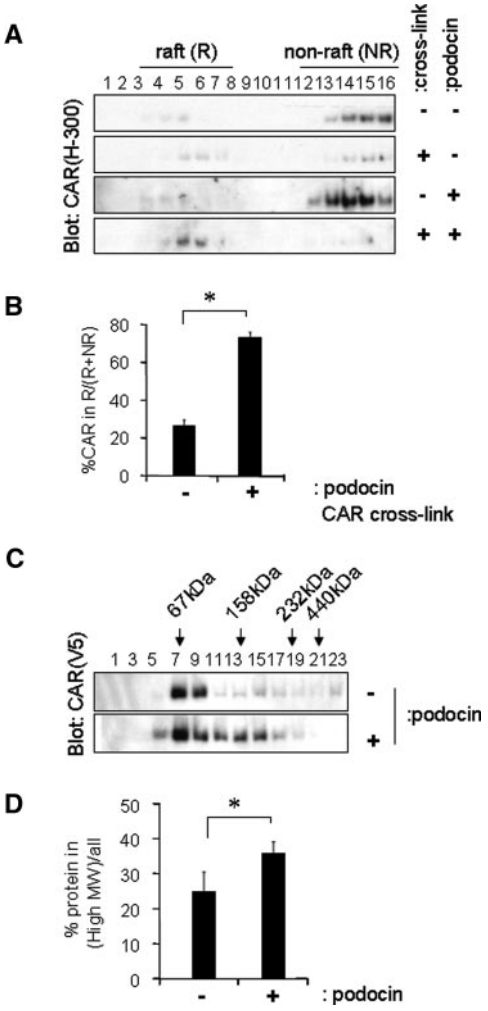

Figure 6. Raft partitioning of CAR is enhanced by antibody-induced cross-linking of CAR and podocin coexpression. (A) The effects of podocin coexpression and CAR ectodomain cross-linking on the raft partitioning of CAR were examined by the floating assay using 0.2% Triton-X100 resistant membrane preparations. Either podocin coexpression or cross-linking alone did not largely influence the raft affinity of CAR. Both treatments synergistically augment raft association of CAR. Raft fractions (R) are separated from nonraft (NR) fractions by the sucrose density gradient centrifugation of 0.2% TX-insoluble material. CAR was detected by a polyclonal antibody directed against the ectodomain of CAR (H-300). The detailed methods of raft isolation are provided in Supplementary Figure 2. (B) Proportion of raft-associated CAR (R) in the total amount of proteins (R+NR) in all fractions is quantified (*$P < 0.01$; $n = 5$). (C) Effects of podocin on oligomerization property of CAR are examined by flotation on velocity gradient centrifugation. Molecular mass standards are indicated by arrows. (D) Proportion of higher order multimers comprising fractions 11, 13, and 15 (High MW) in the total amount from all fractions is shown (*$P < 0.05$; $n = 5$).

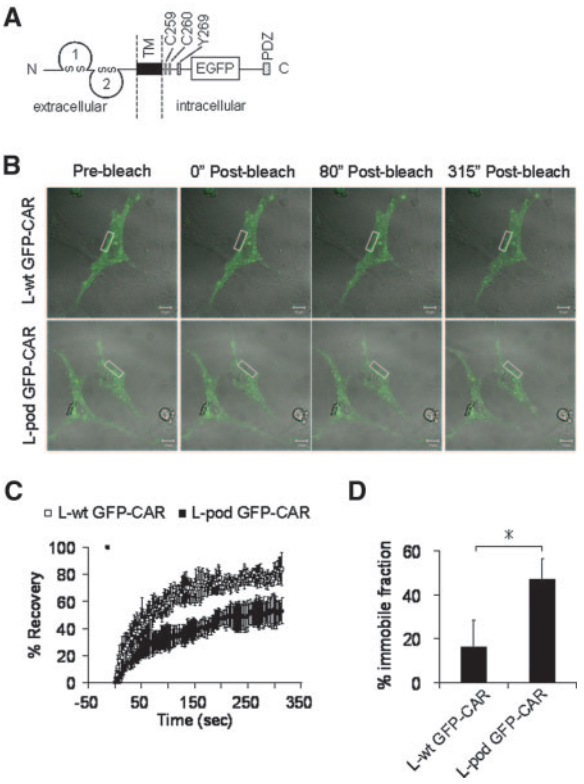

Figure 7. Podocin restricts the lateral diffusion of green fluorescence protein (GFP)-CAR in living mouse L cells. (A) Membrane model of GFP-CAR. GFP is inserted just underneath the TM domain of CAR, leaving an essential cytoplasmic motif intact: Putative palmitoylation sites (Cys 259, 260), tyrosine phosphorylation site (Tyr 269), and PDZ binding motif (Ser-Ile-Val 363 to 365). (B) Merged images from bright-field and fluorescence observations of L cells expressing GFP-CAR alone (L-wt GFP-CAR) and those with stable expression of podocin (L-pod GFP-CAR). Fluorescence recovery after photobleach is measured in boxed regions of 15-μm width. Bar = 10 μm. (C) Kinetics of recovery of L-wt GFP-CAR (□) and L-pod GFP-CAR (■) cells. Each bar shows the mean ± SEM from six cells from three individual experiments. (D) The calculated percentages of the immobile fraction.

DISCUSSION

Our data provide evidence that CAR is assembled and organized as a multiprotein complex *via* membrane rafts in association with podocin and ZO-1. The transmembrane components for the podocyte TJ complex have remained an open question. Neither occludin nor claudin has been detected in the podocytes, whereas other Ig-like proteins, including nephrin and JAM4, have never been evident at the TJ.[21] The N-terminus Ig-like domain of CAR forms homodimers,[22] suggesting that the initial cell–cell recognition is mediated by its homodimerization *in vivo*. However, such "head-to-head" homodimerization does not normally occur at the SD because the ectodomain of CAR, consisting of just two Ig domains, is not long enough to bridge the slit gap (20 to 50 nm). Therefore, engagement of the CAR ectodomains in *trans* occurs only when the opposing membranes come into close proximity after injury. The cytoplasmic tail of CAR has a putative palmitoylation site (Cys at 259 and 260) that facilitates sequestration of rafts lipid[23] and a putative tyrosine phosphorylation site

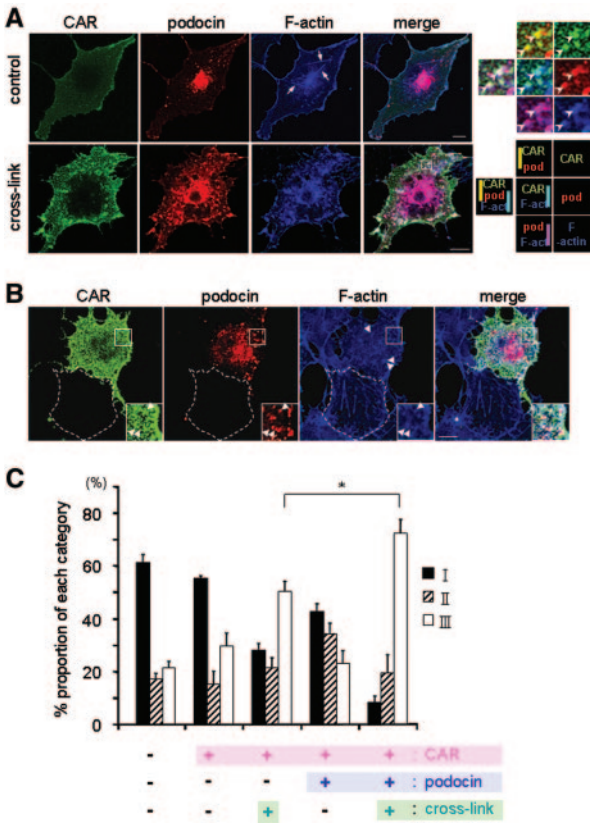

Figure 8. Clustered CAR induces podocin recruitment and F-actin reorganization. (A) Clustered CAR recruited podocin to the actin spots. Upon cross-linking CAR in COS-7 cells coexpressing CAR (green) and podocin (red), actin filaments are reorganized from a filament-like (top, arrows) to discrete punctate pattern (bottom), and podocin is recruited to the spots. Actin filament is visualized by phalloidin (blue). Bars = 10 μm. (B) Clustered CAR induced actin reorganization in association with podocin. White dashed lines denote the contour of untransfected cells. Note that cells devoid of CAR have normal bundle-like stress-fiber distribution even upon cross-linking of CAR. Insets show higher magnification of boxed portion. Arrowheads denote the punctate structures where actin is reorganized in association with CAR and podocin. (C) Quantitative analysis of actin reorganization. The images were binned into three main morphologic subtypes by inspection in terms of actin filament distribution: (I) Predominant stress fibers with few or no actin spots, (II) stress fibers mixed with focal actin spots, and (III) remarkable focal actin spots with loss of stress fibers. The diagrams show the means ± SEM of the distribution of the three phenotypes. The percentage of cells falling into the respective categories was based on more than 80 cell profiles from five independent experiments, thereby ensuring objectivity and reproducibility of the scoring. $*P < 0.01$.

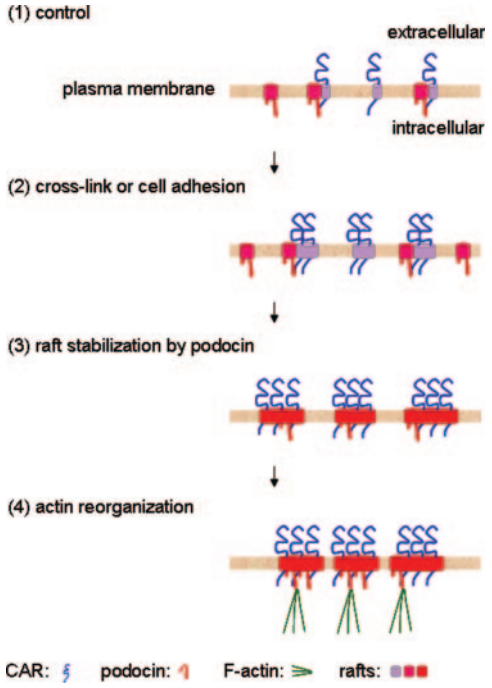

Figure 9. Model illustrating a TJ complex assembly mediated by podocin. CAR and podocin normally reside within individual raft microdomains, with a certain proportion (30 to 40%) being sorted as preassembled CAR/podocin hetero-oligomer complexes. These membrane domains are small and highly dispersed at the cell surface, thereby representing "nonfunctional" or "inactive" microdomains. Antibody-mediated clustering induces the formation of "active" microdomains through the coalescence of neighboring lipid rafts. Such processes selectively recruit and sequester specific sets of interacting partners needed for TJ formation. The properties of podocin such as oligomerization and its high lipid affinity enhance raft association of CAR. Thus, podocin facilitates sequestration of CAR and its downstream signaling molecules central to actin reorganization (*e.g.*, Fyn). In this way, podocin facilitates the efficient conversion of a cell adhesion signal into remodeling of cellular architecture.

(Tyr 269). These features of CAR favor its ability to form a signaling platform that attracts specific sets of raft-associated signaling molecules (*e.g.*, Src-family kinases[7,24]). It is therefore conceivable that CAR integrates the initial cell recognition signal into morphologic reorganization and serves as the initial priming of nascent cell junction formation. CAR–podocin complexes would be implicated in the formation of cell–cell junctions of the nephrotic foot process. However, the physiologic relevance needs to be further evaluated by other approaches such as tissue- and stage-specific knockouts.[25]

Podocin enhances raft association of CAR by promoting its oligomerization in an analogous mechanism to that reported for the other raft proteins.[17] Podocin forms a large oligomeric complex,[5] and its raft association is stabilized in part *via* its C-terminus containing a prohibitin homology domain, reportedly important for lipid–protein interactions.[26] These properties facilitate the ability of podocin as a raft organizer that sequestrates CAR into the rafts, eventually facilitating intimate contacts between signaling molecules by minimizing diffusion of binding partners. Because podocytes have a huge surface area reflecting numerous interdigitating processes, podocin-mediated sequestration of TJ components seems to be physiologically relevant.

We demonstrated that clustering of CAR induces the formation of focal actin spots and concomitant recruitment of podocin. Together with the previous observation that CD2AP localizes the actin spots,[27] our data suggest that podocin may serve as a scaffold that links the membrane complexes to the cytoskeleton. In the rat PAN model, drastic actin reorganization was reported in the foot processes after TJ assembly.[28] Actin concentrates along junctional complexes and regulates permeability of TJ through its contraction. That foot processes are invariably exposed to the hydrodynamic filtration pressure substantiates a need for reinforcement of TJ complexes by anchoring them to the cytoskeleton. These observations suggest that interactions between the SD complex and the actin cytoskeleton play a crucial role in the regulation of SD integrity and foot process architecture.

Podocin remains associated with the cell–cell junctional complex even in nephrotic podocytes. It might be a secondary or passive process reflecting the close structural and developmental relationship between the TJ and SD. During glomerular development, the SD is thought to have originated from apically located TJ in prepodocytes and to have replaced the TJ in mature podocytes.[2,10] The premature, differentiating podocytes bear a number of morphologic characteristics of the nephrotic podocytes.[10,12] Effacement or retraction may represent a "simplification" and "dedifferentiation" to a more primitive organization and represent the reversal of normal developmental processes.

Another explanation for podocin localization in TJ complexes is that it represents the adaptive or reparative responses to the nephrotic condition and injury.[8,29] In podocin-null mice,[30] foot processes develop normally and TJ-like structures are visible, suggesting that podocin is not absolutely necessary to form the immature cell–cell junctions. Notably, the mice lack any SD at birth and develop severe cell damage during the next 7 d and die from renal failure at 6 to 7 wk. We therefore speculate that podocin-null podocytes are structurally labile and highly susceptible to injury because of the inability to scaffold the junctional complexes. Given the unusual feature of the foot process, being continuously exposed to the threat of a high hydrostatic pressure, even minor impairment of junctional assembly might thus be sufficient to produce foot process damage. In patients harboring podocin mutations, dysfunctional orchestration of the integrity of multiple junctions may represent the molecular basis of FSGS.

CONCISE METHODS

Constructs, Cells, and Antibodies

The details are provided as supplementary information.

Immunofluorescence Labeling

Surface proteins on living cells were first reacted with the primary antibodies or Cholera toxin B subunit–biotin (binds to ganglioside GM1) conjugate at 4°C for 20 min and then further incubated at 12°C for 30 min.[17] The secondary antibodies were applied at 12°C for 1 h, and the cells were permeabilized after fixation.

Immunoelectron Microscopy

The tissues from periodate-lysine-paraformaldehyde–perfused kidneys were placed in the periodate-lysine-paraformaldehyde fixative for 4 h and embedded in hydrophilic methacrylate resin.[13,31] Immunogold labeling of ultrathin cryosections was performed as described previously.[9,21]

Immunoprecipitation and GST Pull-Down

For co-immunoprecipitation studies, transfected COS-7 cells were lysed in RIPA buffer (50 mM Tris-HCl [pH 8.0], 150 mM NaCl, 0.5% sodium deoxycholate, 0.1% SDS, and 1% NP-40). Lysates (500 μg) were rocked at 4°C for 2 h with the appropriate primary antibody. Then 40 μl of protein G–Sepharose beads was added and rocked at 4°C for 1 h.[5]

Flotation Gradient Centrifugation

A detergent-insoluble membrane fraction of COS-7 cells and rat isolated glomeruli was isolated as shown in Supplementary Figure 2.

Velocity Gradient Centrifugation

Transfected COS-7 cells were homogenized in Mes-buffered saline (25 mM Mes [pH 6.5] and 150 mM NaCl). The homogenate was centrifuged at 1000 $\times$ *g* for 10 min, and the supernatant was centrifuged at 200,000 $\times$ *g* for 30 min. The pellet was dissociated in Mes-buffered saline containing 60 mM octyl glucoside. Solubilized material was loaded atop a 5 to 40% linear sucrose gradient and centrifuged at 50,000 rpm for 16 h.

Fluorescence Recovery in Photobleaching Analysis

Bleaching of the outlined regions of interest was done at 37°C with the 488-nm laser line at full power and full transmission for 15 s. The recovery values were normalized by dividing them with the mean prebleach values for each region of interest (LSM Pascal software, Carl Zeiss Inc., Jena, Germany). The mobile fractions were estimated at the time points, where the recovery of fluorescence reached a plateau.

Statistical Analysis

The unpaired *t* test with a $P < 0.05$ was taken as significant.

ACKNOWLEDGMENTS

This work was supported by a Grant in Aid for Scientific Research B 16390245 and C 14571026 from Japan Society for the Promotion of Science.

Part of this article was presented in abstract form at the annual meeting of the American Society of Nephrology; November 12 through 17, 2003; San Diego, CA.

We are grateful to Drs. K. Taguchi, N. Tanimura, K. Kawai, and Y. Taketani for assistance of rafts experiments.

DISCLOSURES

None.

REFERENCES

1. Remuzzi G, Benigni A, Remuzzi A: Mechanisms of progression and regression of renal lesions of chronic nephropathies and diabetes. *J Clin Invest* 116: 288–296, 2006
2. Pavenstadt H, Kriz W, Kretzler M: Cell biology of the glomerular podocyte. *Physiol Rev* 83: 253–307, 2003
3. Kestila M, Lenkkeri U, Mannikko M, Lamerdin J, McCready P, Putaala H, Ruotsalainen V, Morita T, Nissinen M, Herva R, Kashtan CE, Peltonen L, Holmberg C, Olsen A, Tryggvason K: Positionally cloned gene for a novel glomerular protein—nephrin—is mutated in congenital nephrotic syndrome. *Mol Cell* 1: 575–582, 1998
4. Boute N, Gribouval O, Roselli S, Benessy F, Lee H, Fuchshuber A, Dahan K, Gubler MC, Niaudet P, Antignac C: NPHS2, encoding the glomerular protein podocin, is mutated in autosomal recessive steroid-resistant nephrotic syndrome. *Nat Genet* 24: 349–354, 2000
5. Schwarz K, Simons M, Reiser J, Saleem MA, Faul C, Kriz W, Shaw AS, Holzman LB, Mundel P: Podocin, a raft-associated component of the glomerular slit diaphragm, interacts with CD2AP and nephrin. *J Clin Invest* 108: 1621–1629, 2001
6. Parton RG: Caveolae: From ultrastructure to molecular mechanisms. *Nat Rev Mol Cell Biol* 4: 162–167, 2003
7. Simons K, Toomre D: Lipid rafts and signal transduction. *Nat Rev Mol Cell Biol* 1: 31–39, 2000
8. Tryggvason K, Pikkarainen T, Patrakka J: Nck links nephrin to actin in kidney podocytes. *Cell* 125: 221–224, 2006
9. Kurihara H, Anderson JM, Kerjaschki D, Farquhar MG: The altered glomerular filtration slits seen in puromycin aminonucleoside nephrosis and protamine sulfate-treated rats contain the tight junction protein ZO-1. *Am J Pathol* 141: 805–816, 1992
10. Reeves W, Caulfield JP, Farquhar MG: Differentiation of epithelial foot processes and filtration slits: Sequential appearance of occluding junctions, epithelial polyanion, and slit membranes in developing glomeruli. *Lab Invest* 39: 90–100, 1978
11. Lahdenkari AT, Lounatmaa K, Patrakka J, Holmberg C, Wartiovaara J, Kestila M, Koskimies O, Jalanko H: Podocytes are firmly attached to glomerular basement membrane in kidneys with heavy proteinuria. *J Am Soc Nephrol* 15: 2611–2618, 2004
12. Caulfield JP, Reid JJ, Farquhar MG: Alterations of the glomerular epithelium in acute aminonucleoside nephrosis. Evidence for formation of occluding junctions and epithelial cell detachment. *Lab Invest* 34: 43–59, 1976
13. Nagai M, Yaoita E, Yoshida Y, Kuwano R, Nameta M, Ohshiro K, Isome M, Fujinaka H, Suzuki S, Suzuki J, Suzuki H, Yamamoto T: Coxsackie virus and adenovirus receptor, a tight junction membrane protein, is expressed in glomerular podocytes in the kidney. *Lab Invest* 83: 901–911, 2003
14. Bergelson JM, Cunningham JA, Droguett G, Kurt-Jones EA, Krithivas A, Hong JS, Horwitz MS, Crowell RL, Finberg RW: Isolation of a common receptor for Coxsackie B viruses and adenoviruses 2 and 5. *Science* 275: 1320–1323, 1997
15. Cohen CJ, Shieh JT, Pickles RJ, Okegawa T, Hsieh JT, Bergelson JM: The Coxsackie virus and adenovirus receptor is a transmembrane component of the tight junction. *Proc Natl Acad Sci U S A* 98: 15191–15196, 2001
16. Kawachi H, Koike H, Kurihara H, Sakai T, Shimizu F: Cloning of rat homologue of podocin: Expression in proteinuric states and in developing glomeruli. *J Am Soc Nephrol* 14: 46–56, 2003
17. Harder T, Scheiffele P, Verkade P, Simons K: Lipid domain structure of the plasma membrane revealed by patching of membrane components. *J Cell Biol* 141: 929–942, 1998
18. Huber TB, Simons M, Hartleben B, Sernetz L, Schmidts M, Gundlach E, Saleem MA, Walz G, Benzing T: Molecular basis of the functional podocin-nephrin complex: Mutations in the NPHS2 gene disrupt nephrin targeting to lipid raft microdomains. *Hum Mol Genet* 12: 3397–3405, 2003
19. Brown DA, Rose JK: Sorting of GPI-anchored proteins to glycolipid-enriched membrane subdomains during transport to the apical cell surface. *Cell* 68: 533–544, 1992
20. Jones N, Blasutig IM, Eremina V, Ruston JM, Bladt F, Li H, Huang H, Larose L, Li SS, Takano T, Quaggin SE, Pawson T: Nck adaptor proteins link nephrin to the actin cytoskeleton of kidney podocytes. *Nature* 440: 818–823, 2006
21. Hirabayashi S, Mori H, Kansaku A, Kurihara H, Sakai T, Shimizu F, Kawachi H, Hata Y: MAGI-1 is a component of the glomerular slit diaphragm that is tightly associated with nephrin. *Lab Invest* 85: 1528–1543, 2005
22. van Raaij MJ, Chouin E, van der Zandt H, Bergelson JM, Cusack S: Dimeric structure of the coxsackievirus and adenovirus receptor D1 domain at 1.7: A resolution. *Structure* 8: 1147–1155, 2000
23. van't Hof W, Crystal RG: Fatty acid modification of the Coxsackie virus and adenovirus receptor. *J Virol* 76: 6382–6386, 2002
24. Coyne CB, Bergelson JM: Virus-induced Abl and Fyn kinase signals permit Coxsackie virus entry through epithelial tight junctions. *Cell* 124: 119–131, 2006
25. Chen JW, Zhou B, Yu QC, Shin SJ, Jiao K, Schneider MD, Baldwin HS, Bergelson JM: Cardiomyocyte-specific deletion of the Coxsackie virus and adenovirus receptor results in hyperplasia of the embryonic left ventricle and abnormalities of sinuatrial valves. *Circ Res* 98: 923–930, 2006
26. Morrow IC, Rea S, Martin S, Prior IA, Prohaska R, Hancock JF, James DE, Parton RG: Flotillin-1/reggie-2 traffics to surface raft domains via a novel Golgi-independent pathway. Identification of a novel membrane targeting domain and a role for palmitoylation. *J Biol Chem* 277: 48834–48841, 2002
27. Welsch T, Endlich N, Gokce G, Doroshenko E, Simpson JC, Kriz W, Shaw AS, Endlich K: Association of CD2AP with dynamic actin on vesicles in podocytes. *Am J Physiol Renal Physiol* 289: F1134–F1143, 2005
28. Kerjaschki D: Polycation-induced dislocation of slit diaphragms and formation of cell junctions in rat kidney glomeruli: The effects of low temperature, divalent cations, colchicine, and cytochalasin B. *Lab Invest* 39: 430–440, 1978
29. Shankland SJ: The podocyte's response to injury: Role in proteinuria and glomerulosclerosis. *Kidney Int* 69: 2131–2147, 2006
30. Roselli S, Heidet L, Sich M, Henger A, Kretzler M, Gubler MC, Antignac C, Moutkine I, Gribouval O, Benmerah A, Boute N, Benessy F, Attie T: Early glomerular filtration defect and severe renal disease in podocin-deficient mice. *Mol Cell Biol* 38: 550–560, 2004
31. Bendayan M: Double immunocytochemical labeling applying the protein A-gold technique. *J Histochem Cytochem* 30: 81–85, 1982

Supplemental information for this article is available online at http://www.jasn.org/.